Title: Collective synchrony of mating signals modulated by ecological cues and social signals in bioluminescent sea fireflies

Word count: 9943

Authors:
Nicholai M. Hensley[1,4,*], ORCID# 0000-0003-0681-0808
Trevor J. Rivers[2],
Gretchen A. Gerrish[3], ORCID# 0000-0001-6192-5734
Todd H. Oakley[1], ORCID# 0000-0002-4478-915X

Affiliations:
[1]Department of Ecology, Evolution, and Marine Biology, University of California Santa Barbara, Santa Barbara, CA 93106-9620, United States
[2]Department of Ecology and Evolutionary Biology, University of Kansas, Lawrence, KS 66405, United States
[3]Center for Limnology, Trout Lake Station, University of Wisconsin, Madison, Boulder Junction, WI 54512, United States
[4]Current affiliation: Department of Neurobiology and Behavior, Cornell University, Ithaca, NY 14850, United States

*Corresponding author:
Nicholai M. Hensley, email: nikohensley@gmail.com

Abstract:

Individuals often employ simple rules that can emergently synchronise behaviour. Some collective behaviours are intuitively beneficial, but others like mate signalling in leks occur across taxa despite theoretical individual costs. Whether disparate instances of synchronous signalling are similarly organised is unknown, largely due to challenges observing many individuals simultaneously. Recording field collectives and *ex situ* playback experiments, we describe principles of synchronous bioluminescent signals produced by marine ostracods (Crustacea; Luxorina) that seem behaviorally convergent with terrestrial fireflies, and with whom they last shared a common ancestor over 500 mya. Like synchronous fireflies, groups of signalling males use visual cues (intensity and duration of light) to decide when to signal. Individual ostracods also modulate their signal based on the distance to nearest neighbours. During peak darkness, luminescent "waves" of synchronous displays emerge and ripple across the sea floor every ~60 seconds, but such periodicity decays within and between nights after the full moon. Our data reveal these bioluminescent aggregations are sensitive to both ecological and social light sources. Because the function of collective signals is difficult to dissect, evolutionary convergence, like in the synchronous visual displays of diverse arthropods, provides natural replicates to understand the generalities that produce emergent group behaviour.

Keywords:
collective behaviour, synchrony, bioluminescence, Ostracoda, mating signal, sea firefly

Introduction:

Animal collectives perform some of the most striking examples of behaviour observed [1]. Surprisingly, self-organised aggregations can be the emergent product of individuals following simple behavioural rules [2], as opposed to those that require complicated cognition or decision-making to form. Within these groups, individual organisms may use these heuristics at local spatial and temporal scales, influencing their own behaviours. For example, individual birds within a flock simply track a number of neighbours (i.e. topological [3]) or the distance to nearest neighbours (i.e. metric [4]) in order to coordinate individual flight heading and speed during murmurations. The form and strength of these local mechanisms produces variation in the collective.

Beyond how local interactions scale to the level of collective behaviours, collectives may also be responsive to the environment [5]. Understanding how environmental variables shape variation in animal groups is a major goal in understanding collective dynamics [6,7]. For example, calling cicadas are sensitive to environmental light levels, where spatial synchrony within a forest increases when sound amplitude peaks as individuals increase their calling rate during brighter illumination [8]. However, tracking individuals within groups across environments to tackle such questions is only beginning to gain methodological traction. By understanding the balance between which local rules individuals use [9] and environmental effects, we can model variable patterns of collective action like decision making [10], swarming [11], or synchronisation [12,13].

Synchrony is generally considered the proximity in time of animal behaviours [2]. In animal communication, synchronous mate signalling represents an evolutionary paradox: in a classic scenario with males signalling for the attention of females, many males may aggregate and signal closely in space (called “leks”) and time (“sprees”) [14]. Although this cacophony of signals should be able to recruit more females from farther away (i.e. beacon effect hypothesis [15]), increasing the density of signals increases costs like mate competition and may hinder mate choice [16]. Despite these costs, synchronous displays are found in diverse taxa and various modalities [17]. Across arthropods, synchronised behaviours are taxonomically scattered and probably arose multiple times from within groups without synchronous displays, suggesting multiple convergent evolutionary events [18,19]. Although not conclusive, such prolific patterns of convergence may point towards similar evolutionary pressures (i.e. selection for competition, or an adaptive value). Outside the defensive visual displays of lepidopteran caterpillars [20] and vibrations of treehoppers [21], synchronised mating signals are known from choruses of singing orthopterans [22,23] and cicadas [8], the waving claws of fiddler crabs [24,25], and most famously, the glowing, flash bursts of synchronous fireflies found in Southeast Asia and the Americas [26,27]. These fireflies differ from their non-synchronous relatives, and as in other collective behaviours, seem to use local rules such as responding to the timing [28,29] of visual neighbours [27], which produces emergent synchrony. Here, we add to the collection of synchronous visual displays by documenting the collective bioluminescent behaviours of shallow-water ostracods that show extreme synchrony [30]. By characterising this charismatic and independently evolved behaviour, we propose that luxorine sea fireflies [31] are an excellent system to study the causes and consequences of collective signalling.

Ostracods are millimetre-sized crustaceans found in fresh and marine waters, and many species possess a number of specialised adaptations such as thermophilia [32], desiccation-resistant resting eggs [33], or bioluminescence [34]. Most known species within the subtribe Luxorina, almost exclusively found in the reefs and seagrass beds of the Caribbean Sea [35,36], create distinct patterns of

bioluminescence using packages of protein and substrate secreted into the water to attract females [37–39]. Females use these species-specific displays to orient and swim towards males [40,41], never flashing back. However, males also readily and rapidly switch behavioural tactics based on their proximity to the displays of other males, as well as the density of competitors: in the species *Photeros annecohenae [42,43]* males will either begin to display in close proximity and time to another male (termed "entrainment") or sneak on the display train of another male by following along without producing light [44]. Signalling activity of a population is coincident with levels of available darkness during the lunar cycle [45], indicating that both social and ecological factors are important in modulating individual signalling behaviour in ostracod species.

To investigate the role of ecological and social factors in shaping collective behaviour, we performed *in situ* observations and *ex situ* experiments using a species of ostracods within the genus *Photeros* [31,43]. Currently known by its field designation "EGD" (hereafter), this species lives in seagrass beds off the coast of Panama, and upon first discovery, seemed extremely susceptible to stimulation with external stimuli, like the signals of other males, flashlights, lightning, etc. Anecdotally, many hundreds of animals would initiate their displays within seconds of one another, causing a cascade of light to ripple across the sea floor as new males began their displays synchronously before previous ones faded (Fig. 2). These waves could extend for at least 10 metres, a collective feat for individuals less than 2 mm in size. Although we lacked the ability to accurately measure their spatial extent in the field, we sought to quantify these initial observations. Our data reveal that EGD males are sensitive to the level and timing of external light, resulting in observed waves of collective behaviour. Through field recordings, we also observe that ecological opportunity influences variation in these collectives. By quantifying and comparing these rules with those of other synchronous taxa like fireflies, we can begin to generalise on the shared and unique principles underlying emergent behaviours like collective signalling.

Results:

<u>EGD displays of single males are distinct from other Luxorina species</u>

Like other ostracod species in the subtribe Luxornia, individual males of the species EGD produce spatiotemporally complex signals (Fig. 1A). EGD swims downwards while producing a series of 4 - 8 discrete pulses that last 2 - 5 sec each in a line (Table 1). Because the interpulse intervals are ~1.5 sec long, multiple pulses are visible simultaneously as a male secretes them and continues to swim towards the ocean floor. Compared to other Photeros species, EGD has intermediate pulse durations and interpulse intervals, with durations that are longer than 'flashing' species like *P. morini* [37,46] but much shorter than others. They are also spatially short, with 4 - 8 cm between pulses, and the overall display length is very compact, covering only ~16 cm compared to other *Photeros* that range from 20 – 180 cm (Fig. 1B).

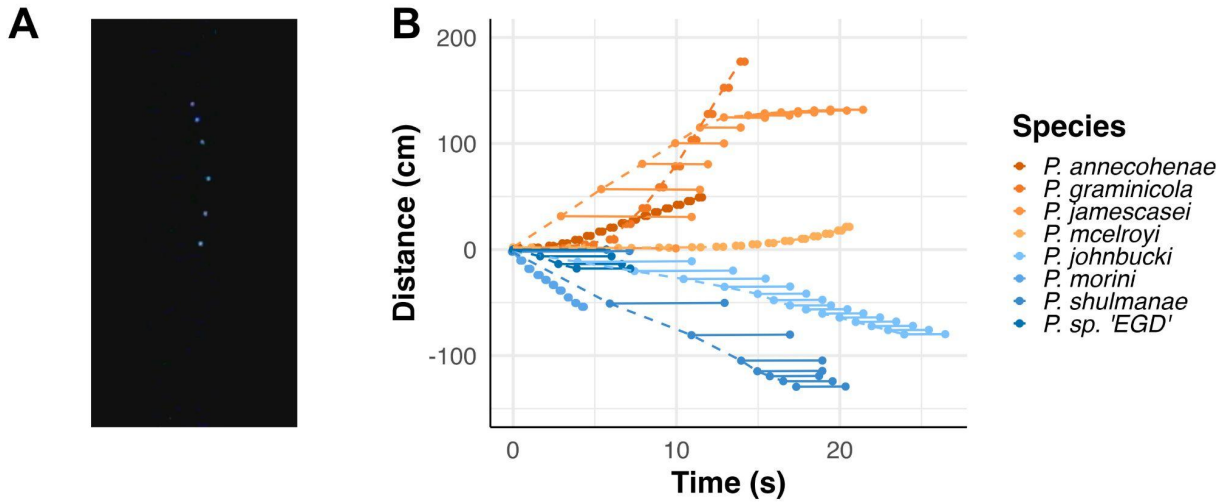

Figure 1. (A) Still frame of a single EGD display train. Filmed on a Canon ME20 with a Canon EF 16-35mm, f/2.8L III USM, inside a Gates Underwater Housing. Image by Presley Adamson and Christy Chamberlain, Monterey Bay Aquarium. (B) Time-distance plots of the average display train characteristics for *Photeros* species. Displays are coloured by species (note EGD in dark blue), with solid, horizontal lines representing the beginning and end of single pulses. Dashed lines connect the start of different pulses within the same display. Species are coloured and separated by whether pulses propagate downwards (blues) or upwards (oranges) over time within a display. Other species data reproduced from [37].

Table 1. Display characteristics of EGD displays from a combination of stereoscopic and single camera recordings *in situ*. All temporal aspects of a display (duration, interpulse interval) are in ms. Distance metrics are in cm. Intensity is relative and normalised to the first pulse within a display train. Interpulse intervals and distances begin between pulse 1 and 2. Replicates per measurement are in parentheses, *N*.

Average display train characteristics		
	Mean ± s.e.m (N)	Max
Pulses per train	4.67 ± 0.465 (15)	8
Vertical train length (cm)	15.8 ± 6.88 (4)	17.8
Train duration (ms)	16,017 ± 2,977 (8)	31,500

Average display trait characteristics by pulse number				
Pulse number	Intensity (% of pulse 1) (N)	Duration (ms) (N)	Interpulse interval (ms) (N)	Interpulse distance (vertical; cm) (N)
1	100 (3)	5,711 ± 527 (8)		
2	68 ± 15.9 (3)	4,367 ± 501 (8)	1,658 ± 154 (8)	6.34 ± 0.982 (4)
3	55.4 ± 1.5 (2)	3,892 ± 618 (8)	1,112 ± 76.1 (8)	7.29 ± 1.25 (4)
4	48.4 (1)	3,279 ± 625 (8)	1,125 ± 70.9 (8)	4.28 ± 0.332 (2)
5	32.5 (1)	3,347 ± 560 (5)	1,093 ± 103 (5)	*
6	1.45 (1)	2,658 ± 621 (4)	1,442 ± 88.6 (4)	*
7	*	2,700 ± 700 (2)	1,217 ± 117 (2)	*
8	*	2,350 ± 1,183 (2)	1,483 ± 150 (2)	*

* no data available

Measures without s.e.m. could not be calculated due to sample size or measurement type

Emergent behaviour *in situ* is evident and timescales correspond to ambient, nightly light cues

Over the course of each night in the grass bed (Fig. 2), the time between waves increases as minutes past nautical twilight increase (Table 2; data not shown). The signalling niche of ostracods is typically nautical twilight, the time of night after sunset and before moon rise where the brightest natural illumination is starlight [40,45]. Thus, within a night, the number of collective displays peaks ~45 minutes after sunset (Fig. 3A) and decreases subsequently. The magnitude of this decrease differed between field seasons, likely due to the smaller number of collective events in 2018 compared to 2022 (Table 2).

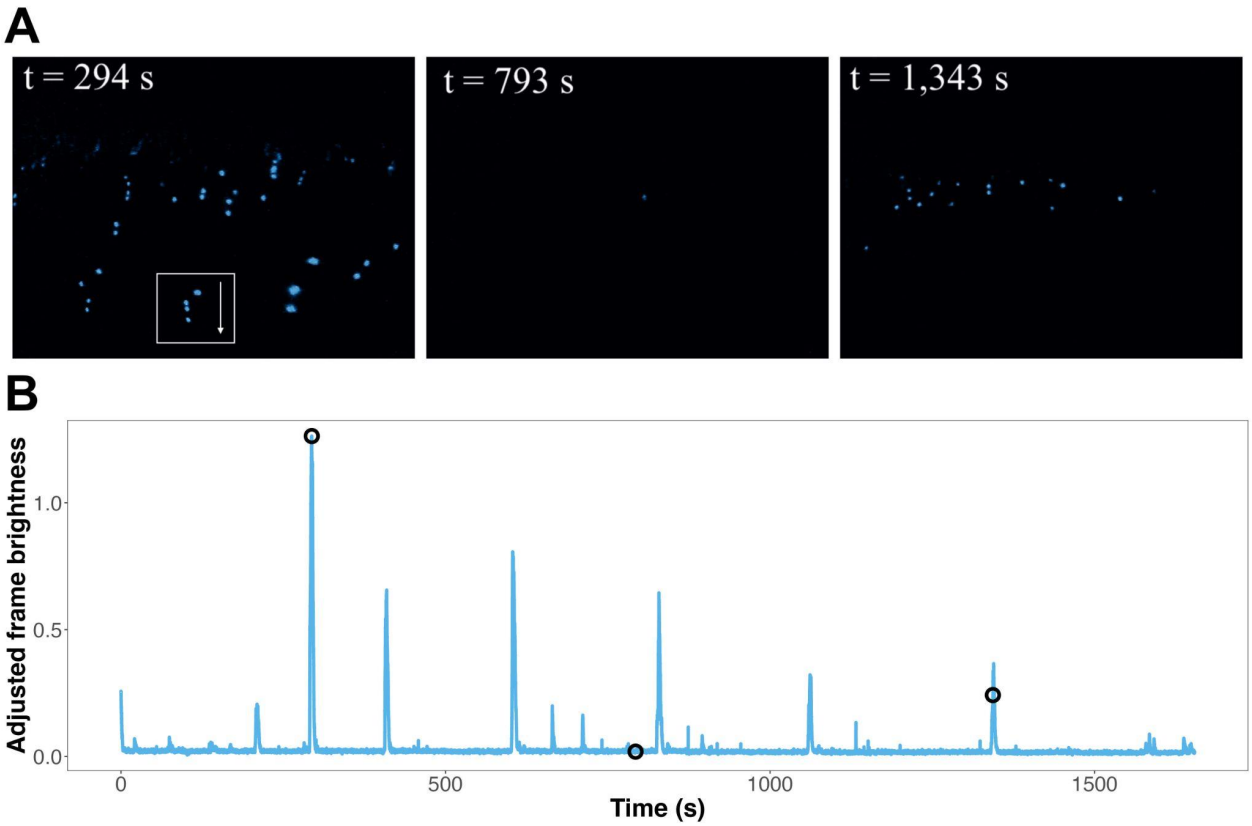

Figure 2. (A) Three video frames (false colour) of EGD signals captured using a WATEC 910HX camera in a custom underwater housing for ~30 min. during a single night of observation, showing bouts of collective behaviour in the wild. From left to right: peak, during an interwave interval, and a smaller, more distant wave. Inset in (A) highlights the display of a single male, seminal to Fig. 1A, with an added arrow to indicate the swimming direction as inferred from the propagation of subsequent pulses over time. (B) Brightness summed across all pixels per frame over time and adjusted with a gamma correction per frame for changes in dynamic sensitivity. Black circles correspond to time points in (A) from left to right.

Table 2. Linear model results predicting the time between collective events by the # of days after the full moon, the year of the field season, the # of minutes after sunset, and their interaction.

		Time between collective events (s)			
Predictors	*Estimates*	*CI*	*Statistic*	*p*	*df*

(Intercept)	-338.67	-482.17 – -195.17	-4.65	**<0.001**	224
# days after full moon	5.3	1.36 – 9.24	2.65	**0.009**	224
Year [2022]	151.81	-5.58 – 309.20	1.9	0.059	224
# minutes post sunset	9.53	6.82 – 12.25	6.92	**<0.001**	224
Year x # min. post sunset	-4.33	-7.25 – -1.41	-2.92	**0.004**	224
Observations	229				
R^2 / R^2 adjusted	0.438 / 0.428				

Between nights, timing between emergent waves is positively correlated with the number of days since the full moon (Fig. 3B, Table 2). As the length of nautical twilight increases during the lunar cycle, the length of time between each subsequent bout of collective signalling also increases. This results in the number of emergent waves decreasing on nights progressively further after the full moon, which again differed between years sampled. Because our sampling window was limited to 1 hour each night, we cannot conclude that the total number of waves during the entire night is greater on days closer to the full moon but we do observe this pattern (Fig 3B, marginal histogram). Thus we limit our analysis to the rate of collective events in a standardised observation window.

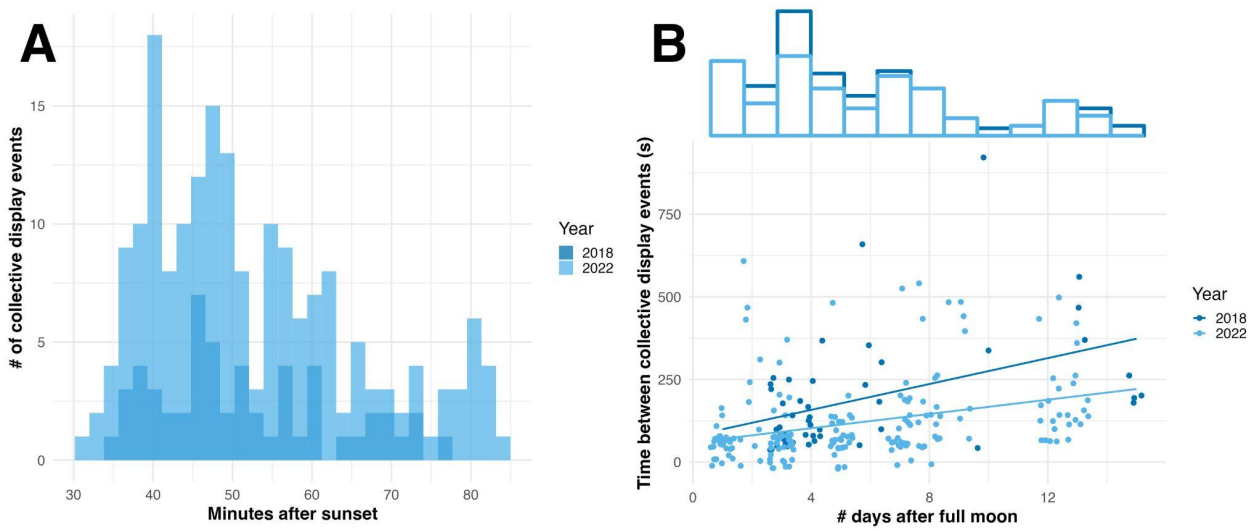

Figure 3. Available nighttime darkness limits the signalling niche within (A) a night and (B) a lunar cycle. (A) Count (y-axis) of the number of collective behavioural events across two field seasons shows that they decrease later into the night (x-axis), as nautical twilight ends. (B) Scatterplot of time between collective display events over a lunar cycle for two field seasons, with a marginal histogram depicting the total number of collective events per night. Time between events increases days out from the full moon. Year of field season indicated by shade: 2018 (dark), 2022 (light). Regression lines are demonstrative; see Table 2 for details of model fit. Data are jittered for visualisation.

<u>Collective and individual responses to timing and brightness *ex situ* correspond to social stimuli</u>

Although apparent to an observer *in situ*, we sought to quantify the level of synchrony between displays in collective behaviours. By placing 100 male animals into aquaria *ex situ*, we could observe waves of displays emerge in a semi-natural habitat (Fig. 4A, independent Trials 1 - 4). The waves are

represented as distinct bars in Fig. 4A, made of 10-15 males displaying within seconds of each other, and with periods of darkness across the entire tank for a minute or more before another set of 10-15 displays erupts. Displays are clustered in space and time (Fig. 4C), and more than would be expected by chance: when compared to a null Poisson distribution of randomly occurring signals at the same mean rate, we see that natural waves have an excess number of signals occurring per second (Fig. 4B). However, this pattern is variable. When using Z and T statistics to compare our observed signal distributions to a null expectation (modified from [47]), we reject the null for all tests except the Z tests for Trials 2 and 3 (Fig. 4B). Next, we explore potential mechanisms that contribute to this variation in synchrony.

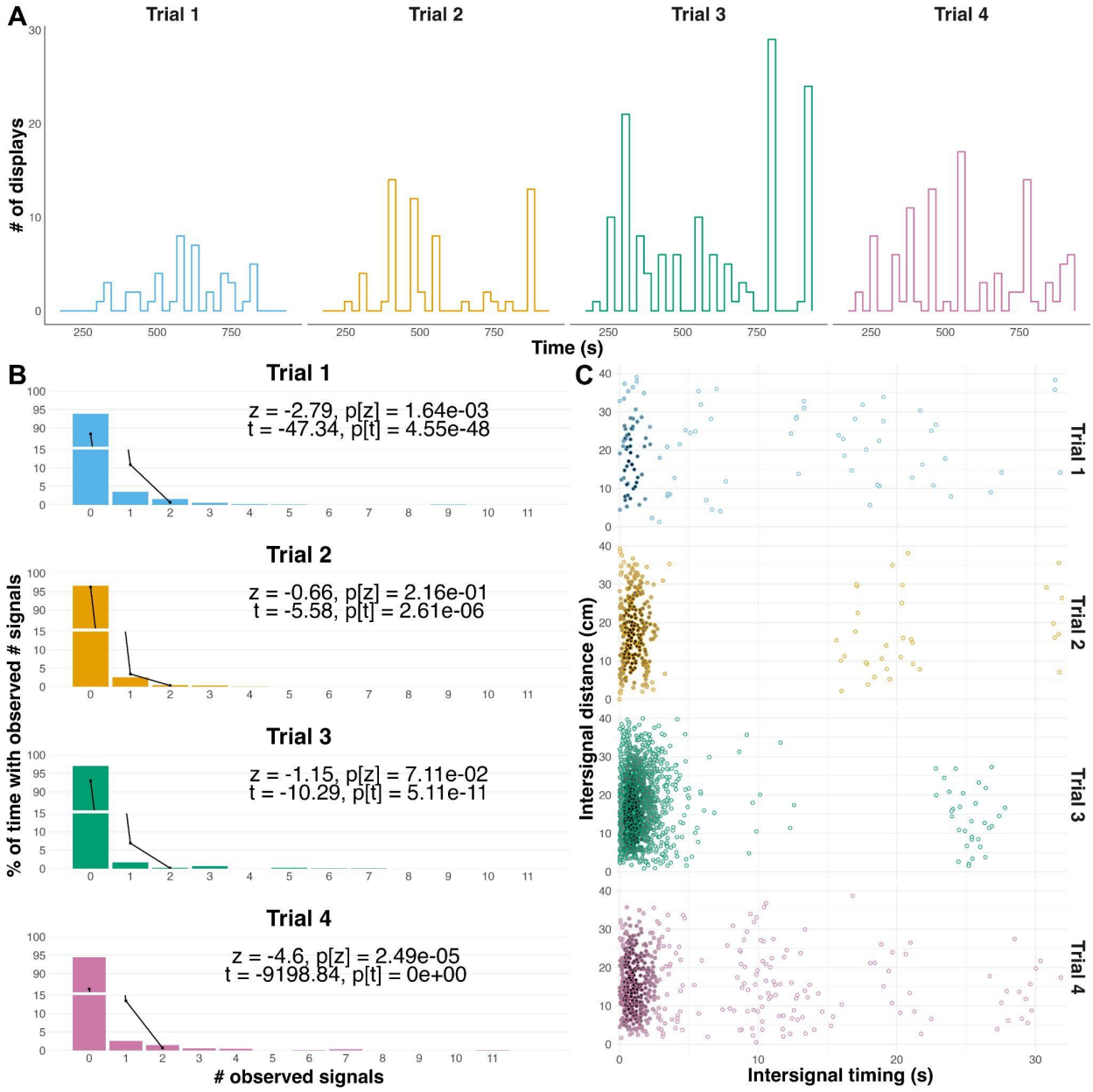

Figure 4. Spatiotemporally annotated sea firefly displays from aquaria during 15 min. observation periods (A) Histograms of the number of observed displays over time for 4 separate trials, each with 100 males per tank. (B) Observed number of signals per second (coloured bars) compared to the null poisson expectation given the same rate of signal production (black line). Note the break in the y-axis. Z and T statistics with accompanying p-values for each trial, as in [47]. (C) Scatterplot of pairwise signal differences in timing (x-axis) and space (y-axis) show periodic clustering. Comparisons are limited to a maximum of 31 sec, the longest any single display could persist in the environment for a conspecific response (see Table 1). Data are jittered for visualisation and coloured by density (darker = more dense).

In *ex situ* experiments, *Photeros* EGD demonstrates differing responses to variation in the brightness and duration of incoming stimuli (Fig. 5, Fig. SX). Collectively, the highest number of animals respond when the stimulus is 4-6 sec long, with a lower number responding to stimuli shorter or longer in duration (Fig. 5A, Fig. S3, Table S1). This coincides well with the duration of the first pulses within individual displays (Table 1). Within two of the stimulus duration replicates, we could also record and measure how individuals time their displays with respect to the onset and offset of stimuli. Almost no individuals begin displays before stimulus onset (n = 4, data not shown). Most males initiate their displays directly after stimulus presentation (n = 700, Chi-squared = 859.79, df = 2, $p < 2.2e-16$). When limiting our analysis to response latencies of 2.5 s or less (approximating the average intersignal timing from natural waves, as from Fig. 4C)), we see males respond most quickly after stimuli of intermediate durations (Fig. 5B, Fig. S6, Table S4). Even individuals that begin their displays during a stimulus (n = 197) have increased latencies to initiate a response as the stimulus durations increase and the distance from the stimulus decreases (Fig. 5C, Fig. S5, Table S3). However, males only delay up to ~7.5 s even if the stimulus duration is greater; again, this coincides well with the maximum duration of first pulses within natural displays.

In addition to stimulus duration, EGD groups also show sensitivity in their collective response to stimulus intensity (Fig. S5, Table S2), responding readily to low levels of light. We observe that a relatively low level of light (estimated ~1,319.91 W sr^-1 m^-2 s, see Methods) elicits a maximum group response, and above which there is little increase in the number of responding males. We lack absolute measurements for the brightness of conspecific displays, and therefore cannot compare the intensity of our stimulus to that of ecologically-relevant social stimuli. At least in wavelength, our *ad hoc* stimulus mimics the colour of conspecific displays, with a peak emission frequency (lambda max) at ~450 nm (Fig. S4) for the filtered light, and which is similar to bioluminescent emission spectra from crushed EGD at ~468 nm [39], as well as the visual sensitivity of congeneric luxorine ostracods at ~473 nm [48].

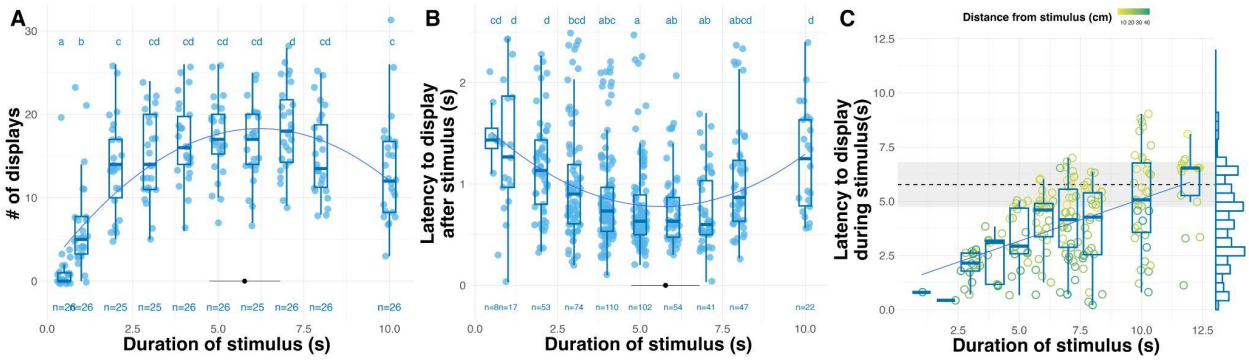

Figure 5. Groups of signalling males show variation in the magnitude of their collective (A) and individual (B,C) responses to stimuli varying in duration. Data are jittered for visualisation. (A) Boxplots with parabolic response curve show that groups are most responsive to stimuli lasting 4-6 seconds in duration. Each datum represents a single experimental trial where we count by eye the number of individual displays produced immediately after stimulus onset. Regression is demonstrative; for model fit, see Table S1. Black datum with whiskers represents the mean and two standard deviations for the duration of the first pulse from observed displays; see Table 1. (B) Boxplots and parabolic responsive curve show that male latency to respond after a stimulus presentation increases at both short and long stimulus durations, with males producing responding signals most quickly at intermediate stimulus durations. Regression is demonstrative; see Table S4 for model fit. Black datum with whiskers represents the mean and two standard deviations for the duration of the first pulse from observed displays; see Table 1. (C) Scatterplot of individuals' latencies to respond during a stimulus increases with longer stimulus durations (x-axis) and closer to the stimulus (lighter = closer). Regression is demonstrative; see Table S3 for model fit. Black, dashed line and grey shaded area represents the mean and two standard deviations for the duration of the first pulse from observed displays; see Table 1. As also seen with the marginal plot, males delay their responses only up to ~7.5 s. For data in (B) and (C), each datum represents the relative timing of a single individual display to the stimulus end or beginning, respectively.

<u>Individuals modulate the number of pulses per display based on stimuli distance</u>

Looking at data from all *ex situ* observations (Fig. 6A) and experiments (Fig. 6D, limited to 90 s post-stimulus), EGD males farther from a conspecific signal produced displays with more discrete pulses per train (Fig. 6B,E). We observe that interdisplay distance describes variation in the timing and latency to display of EGD signals (Fig. 4C, Fig. 5C), as well as the number of pulses within an individual's display (Fig. 6A,B, permutation test, $p = 0.005$; Fig. 6D,E, permutation test, $p = 0$), suggesting that these local interactions are important during collective signalling. In both sets of trials, the time to the next soonest display (i.e. temporal neighbour) also describes variation in the number of pulses per display (Fig. 6C, permutation test, $p = 0$; Fig. 6F, permutation test, $p = 0.001$). And in the experimental trials, the distance to the stimulus also influences the number of pulses per display (Fig. 6G, permutation test, $p = 0$).

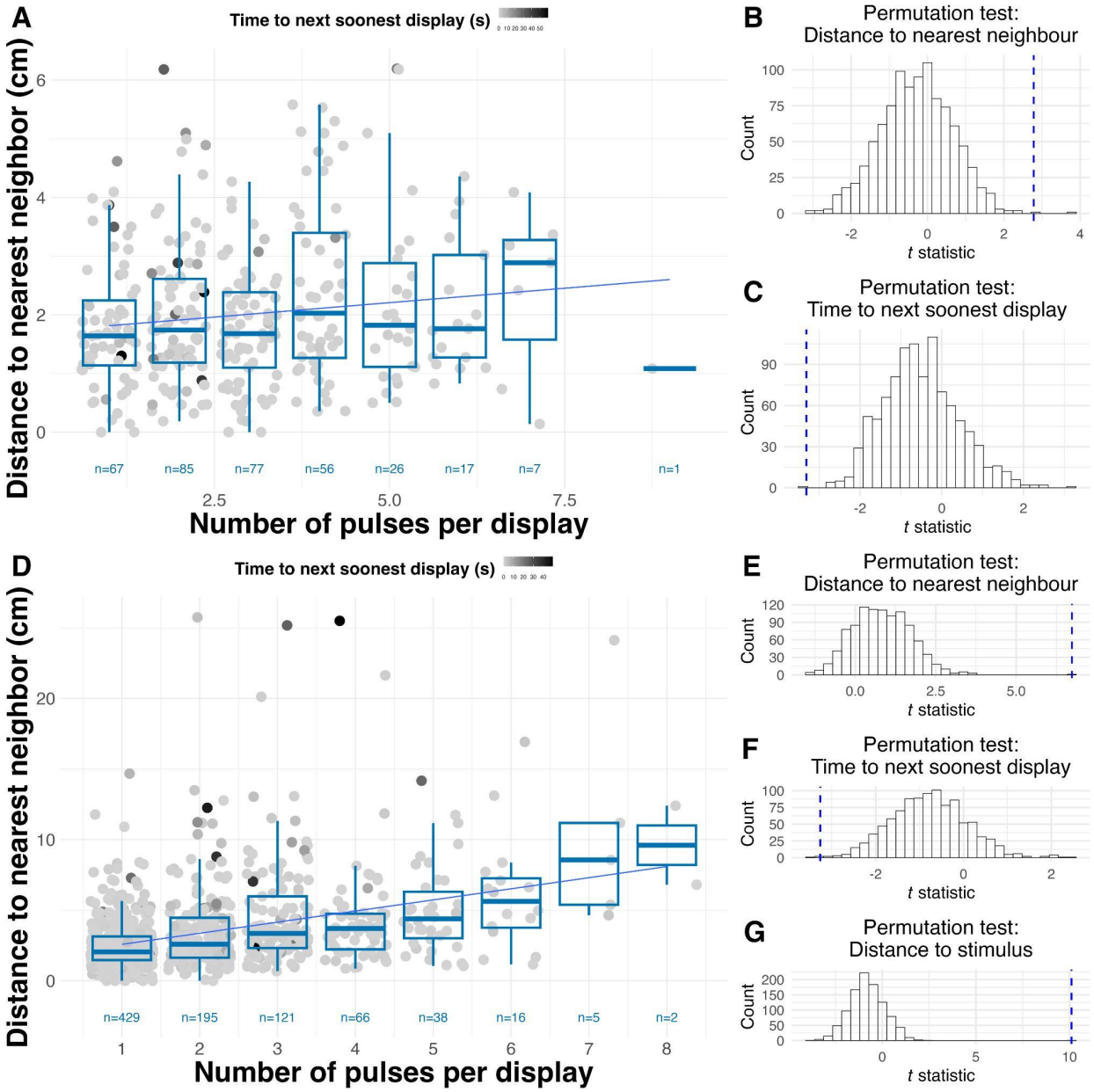

Figure 6. In both (A-C) observational trials and (D-G) experimental trials triggered by an LED stimulus, the distance to the nearest neighbouring male (B,E), and the time to the next soonest display (C,F) influence the number of pulses per display. In experimental trials, we also see that the distance from the stimulus (F) also influences the number of pulses per display. t statistic distributions are the result of 1000 linear models per predictor variable on the number of displays with different permutations of the datasets. Blue dashed lines represent the observed value for each predictor variable. Regression lines in (A,D) are demonstrative.

Discussion:

Collective behaviour is sensitive to social conditions and may be constrained by physical or neurological mechanisms. Our data indicate clearly that a recently discovered species of synchronous sea firefly responds to variation in environmental conditions like the intensity and duration of incoming light.

The magnitude of responses is mediated by variation in these photic stimuli, and other sensory modalities notwithstanding, natural waves of collective behaviour seem to emerge under specific levels of visual stimulation. Our individual-level data reveal that EGD achieves a high level of precision in their signal timing as individuals produce bioluminescent signals in response to a visual stimulus, and with an upper-limit on their response delay. Although variable, sensitivity to external light and intrinsic timing ensures that individuals produce subsequent displays before initiating displays are no longer visible. Understanding variability in these mechanisms will illuminate how synchrony emerges.

Within synchronous waves, there is a lower-limit to the timing between signals, as can be seen by the appearance of relatively consistent periods with few to no displays in the data (Figure 4C). Our field observations (Fig. 2B) and *ex situ* data (Fig. 4A, Fig. S1) coincide with the emergence of wave-like events every ~30 - 60 s. This pattern is likely influenced by some physical constraints on male swimming behaviour, such as needing to swim back up in the water column "silently" after producing a downward train of pulses during a display. However, an intrinsic timing mechanism could also contribute to timing between signalling of different males, as has been proposed for semi-coupled oscillators that model synchronous terrestrial firefly behaviour [12]. Individual latencies to display support the idea that male EGD are able to track temporal changes (Fig. 5B,C). However, whether such a mechanism is appropriate to parameterize a semi-oscillatory model would require data on individuals between and during signalling within a bout of collective behaviour, and which we lack in this study but that could be the subject of future studies in this system.

Signalling males seem to plastically adjust their number of pulses in a display as a function of the distance from conspecific displays or light cues, which we predict if bioluminescent trains are signals to conspecifics, and subject to changes in signalling and/or social environment. Plasticity in male mating behaviours is well documented in the congener *P. annecohenae*, who will change behaviour from luminescent entraining to invisibly sneaking on another male depending on proximity to a leading display train [44]. Closer individuals switch tactics, leading to a reduction in the number of pulses per display due to premature signal abortion by competitors. In EGD, we expect similar behavioural dynamics are occurring in these spree leks, as individuals farther from one another or from a perceived light source create displays with more pulses, perhaps indicating that closer males are rapidly switching tactics from entraining to sneaking as in *P. annecohenae*. Conversely, individuals may be simply terminating their signals based on the local timing cues from neighbours who produce displays with few pulses.

Collective behaviour is also sensitive to ecological cues. The decrease in the frequency and number of collective signalling events in EGD across a lunar cycle supports the hypothesis that the available amount of time of complete darkness during the night is a valuable resource to which luxorine ostracods are attuned [45]. Other ostracod species within this subtribe occupy distinct temporal niches throughout the night when living in complex species assemblages [40], suggesting some mechanism helps each regulate their peak display window. Within the species *P. annecohenae*, there were no discernible patterns of display activity related to long-term lunar activity; adult male behaviour in the wild was best predicted by overall light levels in a night, the availability of which varies with the lunar cycle [45]. This period of darkness may coincide with other cyclical processes, like availability of newly receptive females. Given our experimental results, we believe that EGD are sensitive to short-timescale ecological light levels, similar to its congener *P. annecohenae*, because we were able to manipulate their propensity to display *ex situ* by simply keeping their tanks illuminated despite the time of night or lunar phase. There also may be a circalunar cycle that is important to the timing of EGD reproductive behaviours, which is common in other marine organisms (e.g. corals, spawning annelids, etc.), and which we are not able to

rule out [49]. Similar sampling efforts as done in [45] across a range of lunar phases and paired with manipulative experiments may demonstrate the effects of light sensitivity and intrinsic, clock-like behavioural mechanisms, and how they contribute to behavioural and community diversity.

Just as environmental darkness is an ecological resource, for luminescent organisms ambient light is also a valuable resource - in this case, a signal of their social niche. Correctly identifying and evaluating the social salience of available light levels in the environment can thus be a challenge. Indeed, regardless of signalling modality, filtering out true signals from environmental noise is a sensory and perceptual task that seemingly would have large fitness implications; EGD may have adaptations to help differentiate low-levels of ambient light from dim but increasingly bright conspecific displays. One strategy may be in using mechanisms of temporal integration for recognition, like as a bandpass filter which could ignore changes in light intensity outside a particular temporal frequency. Our data show that EGD are highly attuned to temporal features of stimuli (Fig. 5), and costs of recognition errors may be higher in the temporal domain given the prevalence of other non-salient light cues in the environment such as moonlight, the bioluminescent signals of other organisms (dinoflagellates, cnidarian polyps, syllid worms [50]), and occasionally other ostracod species that occur where two habitat margins overlap (pers. obs), offering a larger opportunity for reproductive interference.

The function, if any, of mass synchrony on such a scale remains to be explored experimentally. Collective signals are known in arthropods, but their adaptive functions can be hard to assess. Some success has been made in fiddler crabs [51] and bees [52], using mathematical models of synchronous insects [53], and recently in a non-arthropod, the sulphur molly [54]. In synchronous fireflies, males benefit from collective signals during mate choice because females respond more [55]; therefore synchrony is thought to aid in species recognition by decreasing visual clutter. However, in fiddler crabs [51] and katydids [53], females prefer leading males, producing increased competition between faster males - thus sexual selection via female precedence preference results in incidental synchrony (an “epiphenomenon”). Previous modelling work indicates that competitive interactions between signallers is sufficient to produce collective dynamics [19,53], however the generalizability of this model has not been vetted. Marine ostracods like EGD have a number of unique attributes that make them more tractable for future studies in these areas: (1) they are abundant, small, and non-seasonal; (2) sexes, lifestages, and signals are easy to differentiate; and (3) they will behave in captivity.

Synchrony may be the result of extreme sexual selection in the form of mate competition. Runaway processes on competitive traits may exaggerate form over evolutionary time (i.e. antler size in red elk [56]). In the case of luminous ostracods like EGD, sensitivity to neighbouring signals as indicated by external light levels may be the target of sexual selection, subsequently leading to increases in the propensity to entrain. Male emergent synchrony could also be an example of bet hedging the benefits of mate signalling with costs in the face of predation. In this scenario, male behaviours are under opposing forces of natural and sexual selection, and males dilute the risk of predation by synchronising while sacrificing some portion of their individual recognition during mate selection. Although we cannot rule out this alternative currently, bioluminescence in ostracods is believed to be an anti-predatory trait [31] and thus synchrony produced from individual bet-hedging seems less likely. As to which of these hypotheses is most explanatory requires testing via manipulative experiments to assay the costs and benefits of different behavioural strategies.

In this work, we have described a unique marine system that is seemingly convergent with terrestrial fireflies in the emergence of synchronous mating signals. Like their aerial arthropod cousins, sea fireflies produce individual luminous mating displays that coalesce into collectives based on local

rules of interaction. One assumption in investigating synchronous mating signals using a comparative framework is that these emergent collective phenomena are heritable. It is difficult to hypothesise about the genetic basis of synchrony (although some work attempts to find neuronal or genetic mechanisms, as referenced in [57]). Rather than solely emergent from plastic responses to the social or ecological environment, variation in the behavioural rules that underlie the emergence of synchrony in each taxon should be transmissible between generations, like sensitivity to conspecific signals, and are both quantifiable and can be linked to the collective properties. These types of behaviours seem more tractable for understanding how synchronous mating systems repeatedly evolve. Being clear about the behavioural mechanisms that produce synchrony in diverse clades, and measuring analogous variables across clades in similar ways will be key in making studies comparable in a phylogenetic framework to understand the evolutionary pressures that produce emergent behaviour [5,58,59].

Methods:

A comment on synchrony versus entrainment in Ostracoda

Although previous work documents spatial clustering with strong temporal entrainment in some ostracod species [43,60], synchrony has never been described. Synchrony is technically distinct from entrainment, and the two are often conflated [61]. In chronobiology, entrainment invokes a mechanism whereby an internal, rhythm-generating oscillator becomes phase coupled to another cyclical process (i.e. tidal, circadian, another organism's oscillatory mechanism, etc.). Previous descriptions of ostracod signalling describe entrainment as "loose synchrony" [37,44], and the term was seemingly used to provide a logical comparison with other synchronous displays like in terrestrial fireflies [62]. However, distinguishing between synchronous behaviours due to entrained, clock-like mechanisms or non-entraining responses requires careful manipulative studies that have not been performed to date within luxorine ostracods. Previous attempts to elicit single displays from individuals, which would be necessary to disambiguate between rhythmic or responsive behaviours, have failed as males seem to require the presence of congeners to display within lab settings [44]. In this study, we attempt to strike a balance between the two terms, but primarily deal with synchrony despite the apparent relevance and previous invocations of entrainment in this system.

Animal Collection and Maintenance

We collected both male and female *Photeros* sp. "EGD" (nightly from 11 - 23 May 2017 and 21 - 26 September 2018, respectively) using baited conical traps [63] placed in the grass beds of Punto Manglar (9.332464, -82.254105) off the coast of Bocas del Toro, Panama. Males were also collected via sweep netting through visible displays. Adult animals were sorted by eye the next day and kept in batches in tupperware with fresh sea water (Gladware 24oz. containers). Each day we checked the health of individuals and changed their sea water; we fed them fish flakes (Seachem NutriDiet MarinePlus Enhanced Marine Flakes with Probiotics) every other day.

Characterising individual EGD displays

EGD displays were measured using two separate systems. Timing characteristics were collected from continuous filming of collective displays during field work in May 2017. Underwater scenes were filmed with a stabilised Sony A7 and Atomos Shogun system in custom underwater housing, as in [64].

From video, we then measured the duration, interpulse interval, and total number of pulses from displays that were contemporaneous but distinct.

Distance measures were collected from continuous filming of collective displays during field work in September 2018. Using two WATEC 910HX cameras at a fixed distance from one another in a custom underwater housing and that simultaneously record the same vantage, we could then calculate the absolute distances (Oakley et al. *in prep.*). From this video, we measured the interpulse distances, and total display length.

To measure the intensity of pulses, we placed multiple individuals in a glass aquarium and recorded their displays using a Hamatsu photomultiplier tube placed perpendicular to and at a fixed distance from the tank. From this time series of intensity over time, we isolated train of peaks that were discrete, decayed continuously without interruption, were grouped in time, and non-overlapping, matching expectations from similar recordings in the congener *P. annecohenae [38]*.

In situ observations

Field observations occurred every 2 - 3 nights after the full moon during 27 September - 10 October 2018 and 13 - 24 July 2022. Directly after the onset of nautical twilight and the first visible wave of collective bioluminescence, a single observer stood in the seagrass and counted the number of events during a 60 min. period. Within the course of a field season, the observer made recordings from the same place in the seagrass bed and facing the same cardinal direction. Displays were considered collective waves if 5 or more individual displays were visible within ~5 s of one another in a 2 m radius from the observer's field of vision.

Ex situ observation and experiments

Experiments occurred nightly from 18 - 22 May 2017 between 2100 hrs and 0300 hrs in the water tables at Bocas del Toro STRI Panama. During the day, 100 male EGD were checked by eye and separated into batches for experiments that night. At ~1800 hrs, we filled tanks with clean sea water to a depth of 15-20 cm. using a standing pipe to cover the drain and set the water level. Each batch of 100 males was placed into a separate tank (dimensions: 100 x 100 cm), with up to 4 tanks being used each night. In order to prevent males from signalling and to simulate the onset of night, we turned on two puck lights set on the edge of each tank to shine white light until we were ready for testing. When we were ready to test, lights would be extinguished, animals were given 20 min. to adapt to darkness, and we observed tanks for 15 minutes before exposing them to any stimulus. Each day after experiments from the night before, tanks were drained and washed with fresh water to remove any animals, and then allowed to air dry until the following night of experiments.

For each stimulus exposure experiment (both intensity and duration types), we used a dive light with white LED lights covered with a blue film as the stimulus, which was the only light source available. Anecdotally, this light source was used to trigger waves of male displays *in situ*, and thus was deemed adequate to elicit a response from captive males in our tank experiments. To use as a stimulus, we connected the LED to an Arduino mini-controller and pre-programmed a range of square-pulse signals to drive the LED on or off. We used a nested design to expose each tank every night tested (deemed a trial) to the full range of conditions within a stimulus type three times each. During each trial, we randomly assigned the order of the test conditions within a tank, and between trials, we randomly assigned the order of testing among tanks. We used Excel to generate four series of random sequences of stimulus conditions and randomly assigned one series to each tank every night. We programmed these four series into the

Arduino code to loop automatically through each stimulus within a series after the initiation of each trial. An observer counted the number of animals that responded to a stimulus by counting the number of unique displays in a tank within 1 minute of the stimulus onset.

Stimuli durations were 500 ms, and 1, 2, 3, 4, 5, 6, 7, 8, 10 s long. Because we co-opted an a*d hoc* stimulus, intensity was not measurable in standardised units during experiments, and may or may not accurately model conspecific or environmental stimuli. Instead, we used a relative percentage of power output to regulate the intensity of the stimulus; by using an Arduino, we could pass up to a maximum voltage output (2 V), which could also be modulated in a standardised manner relative to this maximum. We used stimuli from ~2% to 100% of the electric potential across 10 experiments, and which in Arduino code are expressed in bytes: 5 (1.9% or 0.038 V), 10 (3.9% or 0.078 V), 20 (7.8% or 0.156 V), 30 (11.8% or 0.236 V), 50 (19.6% or 0.392 V), 70 (27.5% or 0.55 V), 90 (35.3% or 0.706 V), 120 (47.1% or 0.942 V), 180 (70.6% or 1.412 V), 255 (100% or 2 V).

Post-hoc measurements indicated that our stimuli were maximally: 966 to 30,117 $W \cdot sr^{-1} \cdot m^{-2}$ for stimuli at 5 to 255 bytes of power, respectively, and measured directly in front of the stimulus (Fig. S4). We measured side-welling spectral irradiance of the LED covered with a blue plastic bag using a fibre-optic spectrometer based on an Ocean Optics USB2000 (Dunedin, FL, USA). We calculated intensity by measuring the irradiance of the stimulus from 300 - 800 nm at different power levels (5, 25, 50, 100, 200, 255 bytes) at three locations in the aquaria, using a 1000 um fibre fitted with a cosine corrector (CC-3) and calibrated with a NIST (National Institute of Standards and Technology) traceable tungsten halogen lamp (LS-1, Ocean Optics), as done previously [65].

For two tank experiments and four 15-min observation periods (Trials 1 - 4), video recordings were available. We filmed tanks obliquely from above, approximating directly overhead, using a Sony A7S with High ISO setting and attached to an Atomos Shogun for video recording in 4K. Videos were exported to Final Cut Pro, and then observers used the software Tracker [66] to record the start time, position of first pulse, and number of pulses per display during the trial or observation window. In the two experimental trials, observers also noted the relative timing of display start times with respect to stimulus start and end time, and total duration.

Data Analysis

Almost all statistical analyses were performed using linear models unless otherwise noted. Specifics for each model are below and can be found in the code (Electronic Supplementary Material). For all our models where possible, we used the 'check_model' function from the package "performance" to visually inspect residuals and check model assumptions. If we tested the presence of interactions or other variables that were subsequently excluded because they were not significant, we used the 'anova' function to compute a chi-squared test and compare the simple model versus the more complex model to decide if explanatory variables should be retained. All data and statistical analyses were performed in R (vers. 3.6.2) with RStudio (vers. 2022.12.0+353). Figure colours from [67,68].

To understand how different timescales influence the observed number of collective display waves, we fit a linear model using OLS of the following construction:

# of collective displays ~ Days after the full moon + Year * Minutes post sunset (Eqn. 1)

Results in Table 1.

To test if the number of responding displays differed among experimental treatments, we used the following models fit with OLS. Although our data are counts, they reasonably met the assumptions of a normal distribution to use linear models:

# of displays ~ poly(Stimulus duration, 2) + Tank/Testing order (Eqn. 2)

# of displays ~ log10(Estimated radiance) + Tank/Testing order + Trial (Eqn. 3)

We nested the order in which tanks were tested within tank identity because we could not test every tank across every level of the testing order. We also included a trial variable to capture variation due to the stimulus presentation order, which was randomised within trials but the same between trials of the same type (see Methods above). Results in Table S1 and S2, respectively.

To test if individual latency to display differed among experimental treatments, we used the following models fit with OLS:

Latency to respond ~ poly(Stimulus duration, 2) + Testing order (Eqn. 4)

Latency to respond ~ Stimulus duration + Testing order + Distance from stimulus (Eqn. 5)

Results in Tables S3 and S4, respectively. For results from Eqn. 2 - 4, we used the estimated marginal means to look for pairwise group differences, as denoted by the letters for each group. Groups that are not statistically different after a Sidak method correction for multiple comparisons.

To show that signals are clustered in time (i.e. synchronised) and space, we used three approaches. First, we measured pairwise differences between signals for either their timing or their spatial distance during a trial. We limited our analysis to signals produced at most within 31 seconds of one another because this is the maximum duration of signals produced in the wild (Table 1), and therefore relevant to the response time of other individuals. We expect to see discrete as opposed to continuous distributions of pairwise differences if signals are synchronised and/or coincident.

Next, to statistically test if displays are synchronised, we compared the expected number of displays per sampling time to the observed number of displays, as from [47]. Because displays are discrete events, we can consider them to occur from a Poisson process. For a given observation trial, we used the total number of observed displays divided by the total time to calculate the given display rate for an observation trial. We then used this rate to simulate a null expectation asking the following question: given a known display rate, how much of our sampling time contains 0,1,2 … *n* or more displays? We can then compare the expected proportion of time (Fig. 4B, black line) with our observations (Fig. 4B, coloured bars).

Lastly, we used two statistical tests from [47]. Briefly, these statistics are goodness-of-fit tests to compare an observed distribution to that of a Poisson distribution that assumes recorded occurrences (i.e. displays) are uncorrelated. Because our data are coded at the level of single displays (each composed of many pulses), and not at the level of flashes within bursts (the analogous situation in terrestrial fireflies, and for which data these tests were devised), we modified the T test to exclude excess correlation in the structure of measured occurrences (see code in ESM). Significant p-values calculated from these tests would reject the null hypothesis that the observed distribution was generated from a Poisson process.

To understand the factors affecting variation in the number of pulses per display, our data did not meet any distribution assumptions in order to use linear models. As such, we used a permutation approach to understand the effect of important variables. We did 1000 permutations per predictor variable, permuting the pairwise distance matrix for each predictor within each trial of the two dataset types (observational, Fig. 6A-C; or experimental; Fig. 6D-G). Because this is computationally intensive, we limited our analysis to understanding three predictor variables: if the nearest neighbours, the next soonest display, or the distance to the stimulus was relevant to describing variation in pulse number. A caveat to these results is that all these metrics have some level of correlation with one-another (Fig. S8, S9). Although our permutation test is robust to such correlations by design, the reported slopes from our actual linear regression (i.e. not from a permuted dataset) may be incorrectly estimated due to these correlations. To generate p-values from our permutation tests, we used the distribution of t-statistics from the permuted linear regressions, which should have a consistent Type I error rate [69].

The following R packages were used to handle, analyse, and visualise all data: tidyverse [70], ggplot2 [71], readxl [72], RColorBrewer [73], ggpmisc [74], ggpubr [75], dplyr [76], ggExtra [77], MASS [78], ggpointdensity [79], tidyr [80], patchwork [81], png [82], spatstat [83], broom [84], stringr [85], ggbreak [86], performance [87], sjPlot [88], jtools [89], emmeans [90], multcomp [91], multcompView [92], scales [93], GGally [94]. See electronics supplementary material for details.

Acknowledgements:
Thanks to Emily A. Ellis, Vanessa Gonzalez, Nick Reda, Wesley Peery, Cheyenne McKinley, and Rebecca M. Varney for field support. And to Daniel Escobar Camacho for measuring the intensity and emission spectra of our *ad hoc* field stimulus. We thank Drs. Rachel Collins and Harilaos Lessios at the Smithsonian Tropical Research Institute (STRI) for their support, as well as members of the STRI Bocas del Toro Field Station, especially Plinio Gondola, Marcos Alvarez, and Felicito Caito for their assistance in completion of this project. We appreciate advice from Elizabeth Hobson on various statistical analysis.

Funding statement:
NMH was supported by the NSF GRFP, NSF PRFB, and a STRI Short-term Fellowship; he received a Sigma Xi Grants in Aid of Research (G20141015722209), a block grant from the Department of Ecology, Evolution, and Marine Biology at UCSB, and a Lerner-Grey Grant for Marine Research from the American Museum of Natural History to partially fund this work. GAG was supported by NSF (#DEB-1457754); THO was supported by NSF (#DEB-1457439). All work was conducted under the auspices of permits obtained from the Panamanian government and provided by MiAmbiente (Permits #SE/A-54-18, #SEX/A-78-18, #ARB-082-2022).

Supplementary Information

Discussion

On variation in the number of pulses per display

Although males differ in the number of pulses in each display train (Fig. S3), we caution against an energetic interpretation of this variation, as we currently have no metric of the physiological demands during signalling nor do we know if there are fitness consequences for variation in the number of pulses during mate choice. Previous work indicates that the energetics of bioluminescent signalling in ostracods may be a relatively small amount of total luminescent ability [95], but this study could not account for the metabolic activity of swimming. From an information theory perspective, an increased number of pulses coincides with a larger 'duty cycle' or relatively more 'on' time, although species differ in the mean and maximum number of pulses per display (Fig. 1B, Table 1; [37,96]). Anecdotally, individuals within the same species found across habitats that vary in depth produce signals of varying pulse number despite high within species stereotypy, suggesting that multiple ecological factors can limit signal form in ostracods like EGD.

Table S1. Results of a linear model describing changes in collective response to variation in stimulus duration (first and second order), tank used (a proxy for group-level effects), and the order in which tanks are tested.

	# of displays		
Predictors	*Estimates*	*CI*	*p*
(Intercept)	8.86	6.48 – 11.23	**<0.001**
Stimulus duration [1st degree]	49.90	40.44 – 59.35	**<0.001**
Stimulus duration [2nd degree]	-58.35	-67.80 – -48.90	**<0.001**
Tank [B]	7.61	3.07 – 12.15	**0.001**
Tank [C]	20.28	13.85 – 26.71	**<0.001**
Tank [D]	16.27	7.32 – 25.21	**<0.001**
Tank [A] × Testing order	1.57	0.75 – 2.39	**<0.001**
Tank [B] × Testing order	-1.31	-3.64 – 1.01	0.267
Tank [C] × Testing order	-5.76	-8.04 – -3.48	**<0.001**
Tank [D] × Testing order	-3.80	-6.24 – -1.36	**0.002**
Observations	257		
R^2 / R^2 adjusted	0.563 / 0.547		

Table S2. Results of a linear model describing changes in collective response to variation in stimulus intensity, tank used (a proxy for group-level effects), and the order in which tanks are tested.

	# of displays		
Predictors	*Estimates*	*CI*	*p*
(Intercept)	1.03	-3.09 – 5.16	0.622
radiance [log10]	4.58	3.40 – 5.76	**<0.001**
Tank [B]	3.14	-1.75 – 8.04	0.207
Tank [C]	10.86	3.46 – 18.26	**0.004**
Tank [D]	3.70	1.21 – 6.19	**0.004**
Trial	-1.11	-1.97 – -0.25	**0.012**
Tank [A] × Testing order	0.97	0.01 – 1.92	**0.047**
Tank [B] × Testing order	2.32	-0.50 – 5.15	0.106
Tank [C] × Testing order	-1.68	-4.46 – 1.10	0.235
Observations	238		
R^2 / R^2 adjusted	0.337 / 0.314		

Table S3. Results of a linear model describing changes in individual latency to signal during stimulus presentation with respect to variation in stimulus duration, tank testing order, and distance from stimulus.

	Latency to respond (s)			
Predictors	*Estimates*	*CI*	*p*	*df*
(Intercept)	3.37	2.42 – 4.32	**<0.001**	193.00
Stimulus duration (s)	0.28	0.20 – 0.35	**<0.001**	193.00
Testing order	0.45	0.22 – 0.68	**<0.001**	193.00
Distance from stimulus (cm)	-0.11	-0.13 – -0.09	**<0.001**	193.00
Observations	197			
R^2 / R^2 adjusted	0.569 / 0.563			

Table S4. Results of a linear model describing changes in individual latency to signal after a stimulus presentation with respect to stimulus duration (first and second order), and the order in which tanks are tested.

	Latency to respond (s)			
Predictors	*Estimates*	*CI*	*p*	*df*
(Intercept)	0.80	0.67 – 0.93	**<0.001**	524.00
Stimulus duration [1st degree]	-1.39	-2.35 – -0.42	**0.005**	524.00
Stimulus duration [2nd degree]	3.98	3.01 – 4.95	**<0.001**	524.00
Testing order	0.06	0.01 – 0.12	**0.033**	524.00
Observations	528			
R^2 / R^2 adjusted	0.121 / 0.116			

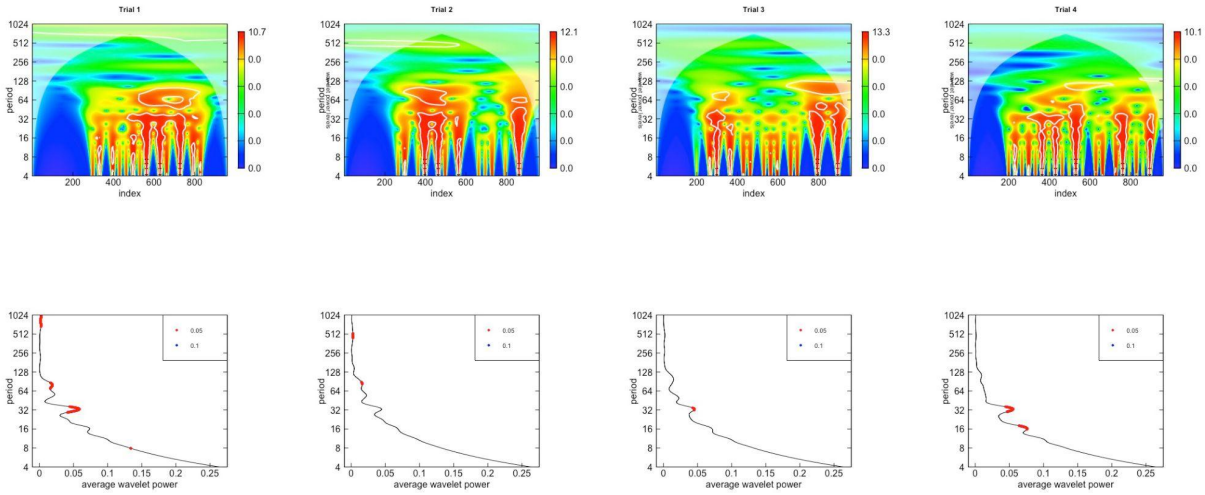

Figure S1. Top row: Wavelet transformation of count observations over time from Trials 1 - 4 of Fig. 4, from left to right respectively. Bottom row: Average wavelet power for each observation trial. Strong signals are found in lower periods for each, with a consistent periodicity every 32 sec, and with secondary periods at 16 and 64 seconds. Periods are measured in seconds, corresponding to the sampling interval of the time series.

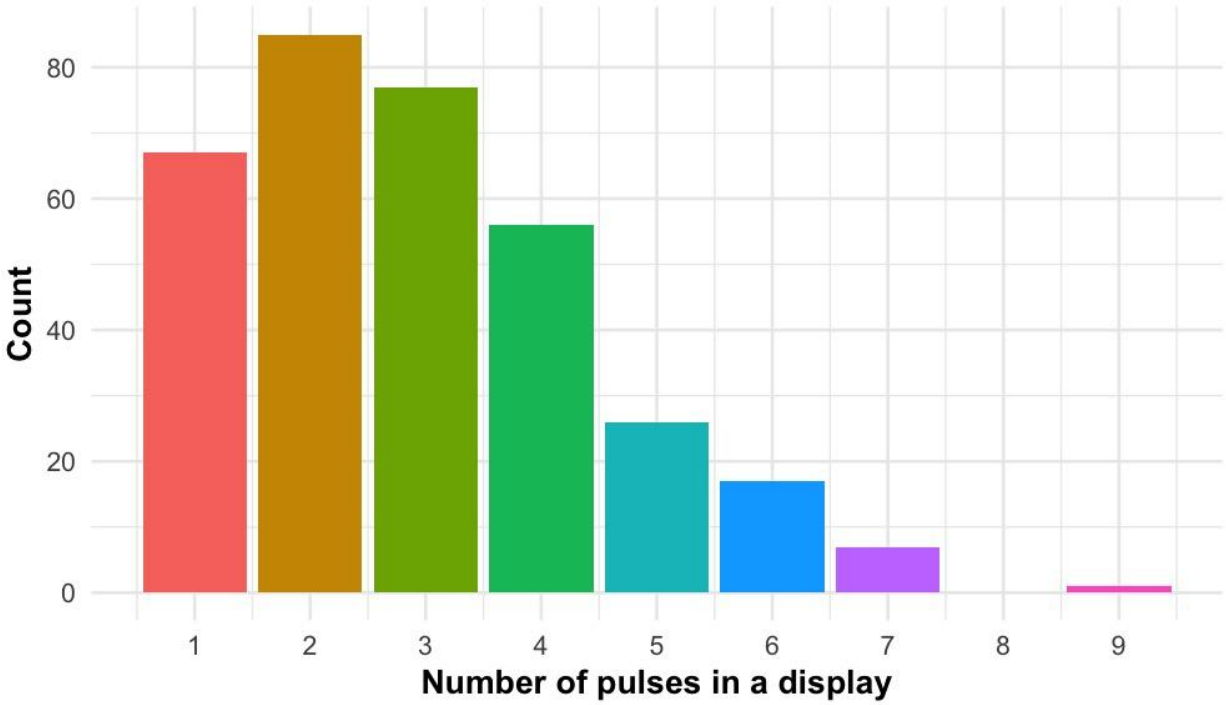

Figure S2. Histogram of variation in pulse number during *ex situ* observations (Trials 1 - 4). Signals with fewer pulses per display are more common, given the animal density (n = 100) and water depth (~20 cm) in the tanks.

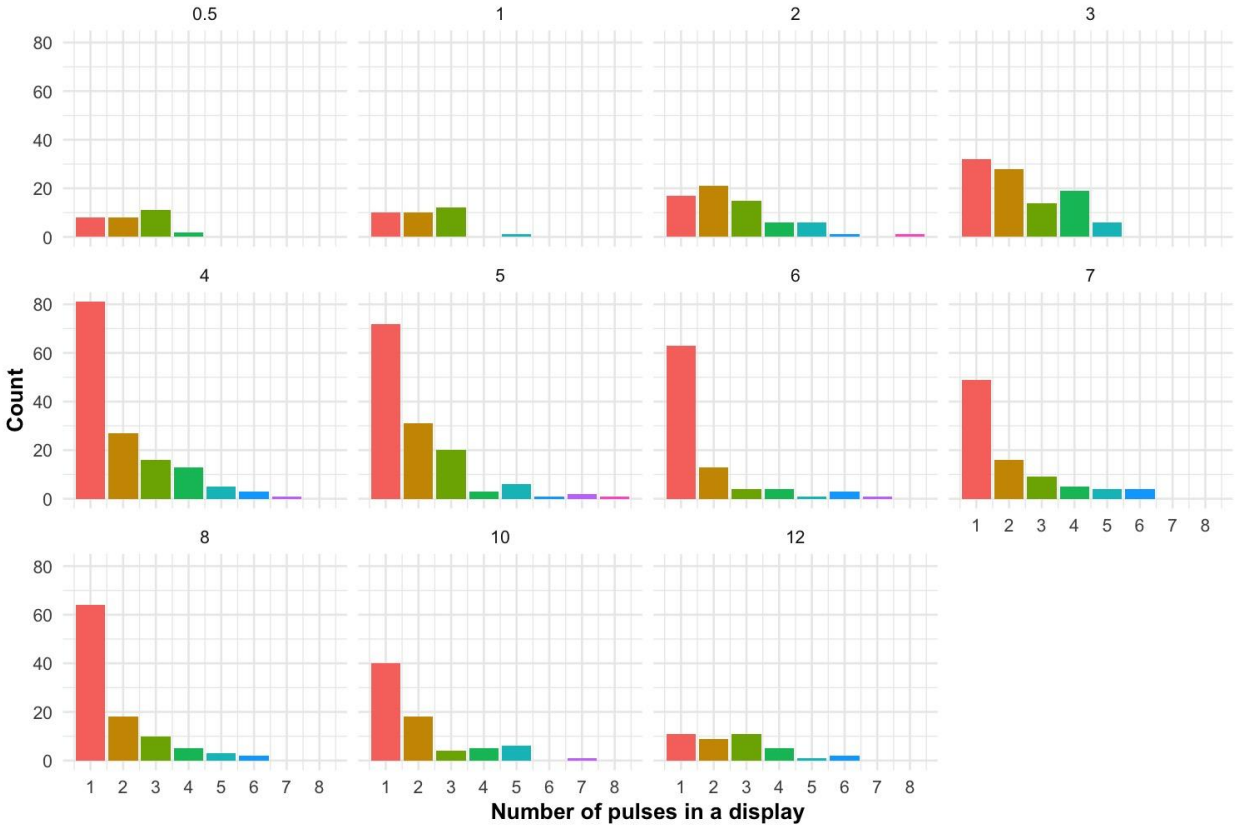

Figure S3. Change in the number of signals and distribution of pulse number per display as a function of the duration of the artificial stimulus. As we only have two annotated trials per stimulus, we cannot perform statistics on these data. We present here to corroborate our observations (Fig. 5A) that intermediate stimulus durations produce more signals.

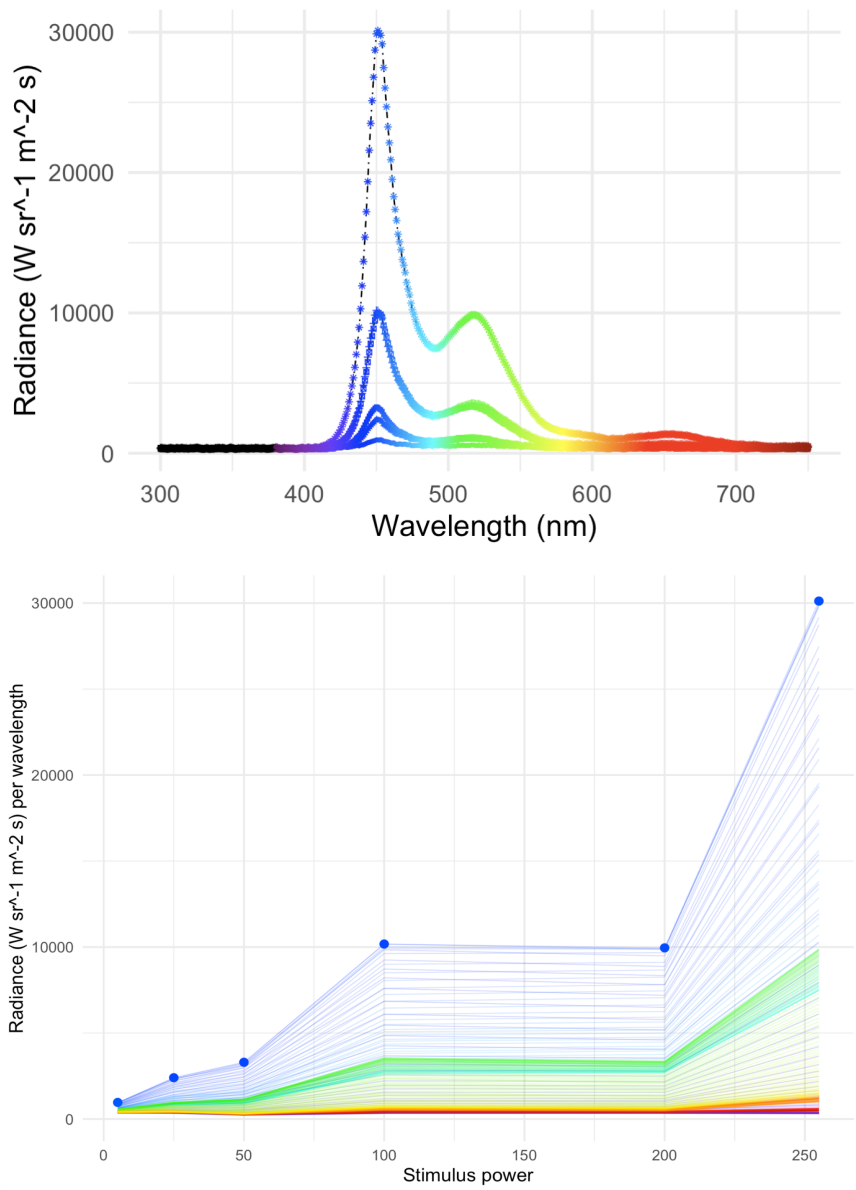

Figure S4. Distribution of radiance intensities across wavelengths for different power levels. Above: radiance by wavelength, with each line corresponding to a different power level. Below: same data as above, but plotted as radiance by power level for every wavelength measured. Therefore, each horizontal line in the plot below represents a vertical slice from the plot above.

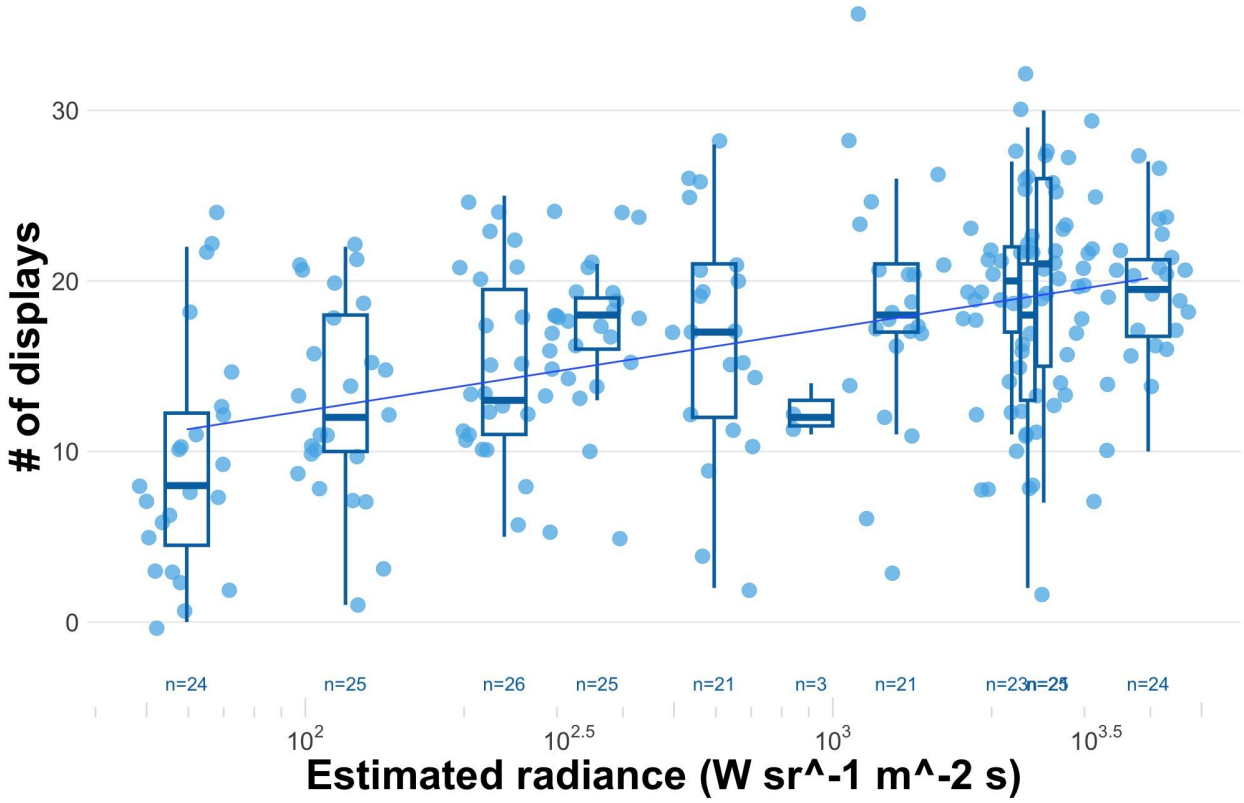

Figure S5. Groups of signalling males show variation in the magnitude of their collective responses to stimuli varying in intensity as measured in radiance. Semi-log plot demonstrates a plateau in response to changes in the stimulus radiance (estimated from data, see Methods and Fig. S3). Data are jittered for visualisation. Each datum represents a single experimental trial where we count by eye the number of individual displays produced immediately after stimulus onset. Regression is demonstrative; for model fit, see Table S2.

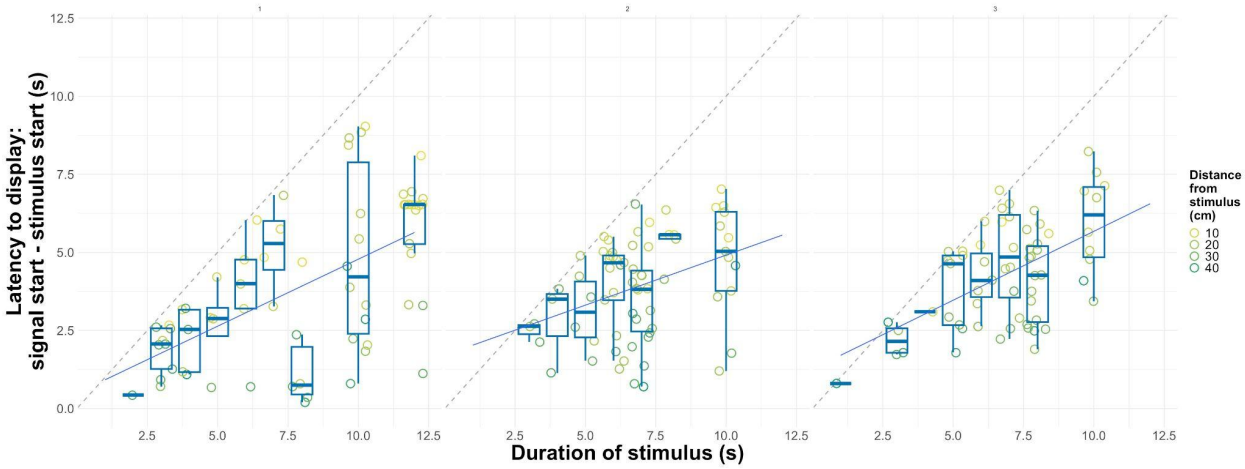

Figure S6. Latency to respond for males creating signals during a stimulus presentation as a function of distance stimulus duration, distance from stimulus, and the testing order of the tank during the night (left to right, panels 1 - 3). Grey dashed lines represent 1:1 line, which we would expect if males simply waited as long as possible until they responded. Instead, we see a regression with lower slope. Regression lines are demonstrative only; for the full model, see Table S3.

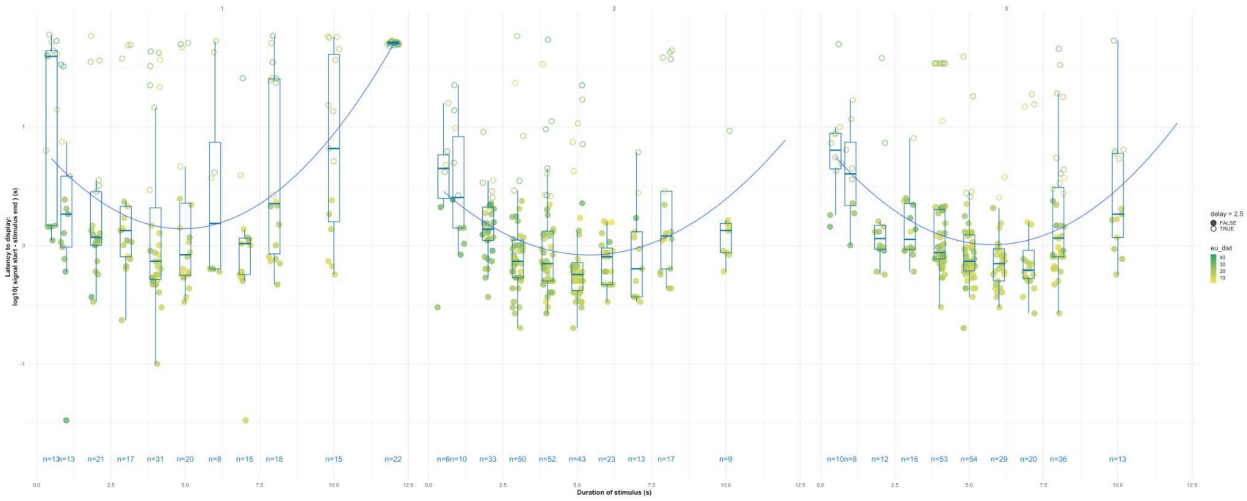

Figure S7. Latency to respond for males creating signals directly after a stimulus presentation ends across variation in stimulus presentation, all data. Note the log transformed y-axis. Pattern is similar to Fig. 5D, which is a dataset restricted to males responding within 2.5 s only (filled data here).

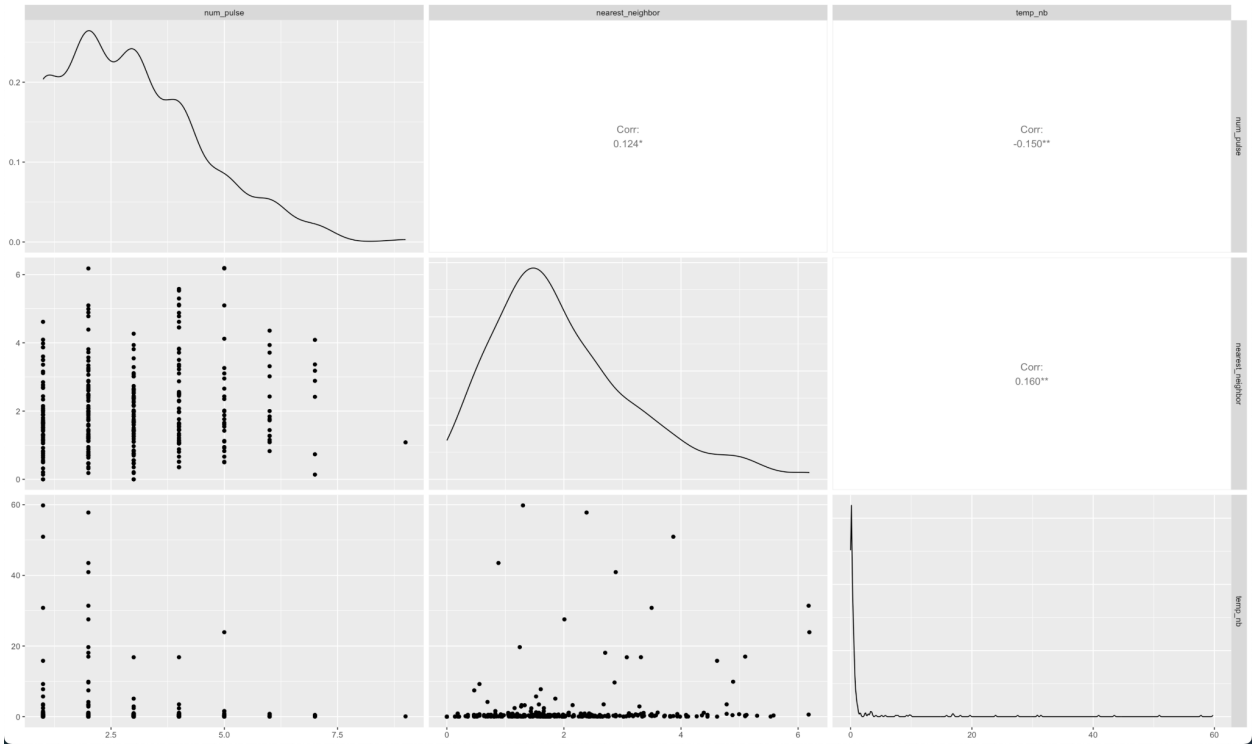

Figure S8. Correlations between time and distance variables in observational trials.

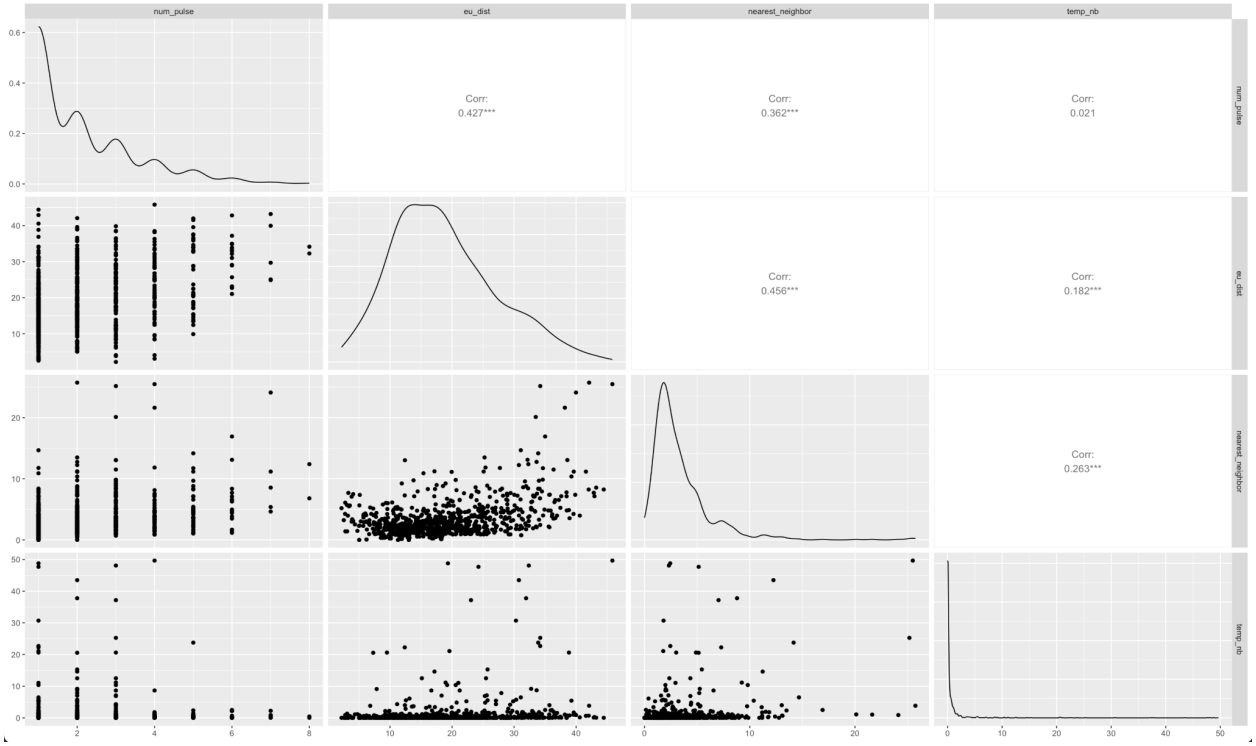

Figure S9. Correlations between time and distance variables in experimental trials.

References:

1. Shishkov O, Peleg O. 2022 Social insects and beyond: The physics of soft, dense invertebrate aggregations. *Collective Intelligence* **1**, 26339137221123758.

2. Sumpter DJT. 2010 *Collective Animal Behavior*. Princeton University Press.

3. Ballerini M *et al.* 2008 Interaction ruling animal collective behavior depends on topological rather than metric distance: evidence from a field study. *Proc. Natl. Acad. Sci. U. S. A.* **105**, 1232–1237.

4. Evangelista DJ, Ray DD, Raja SK, Hedrick TL. 2017 Three-dimensional trajectories and network analyses of group behaviour within chimney swift flocks during approaches to the roost. *Proc. Biol. Sci.* **284**. (doi:10.1098/rspb.2016.2602)

5. Gordon DM. 2014 The ecology of collective behavior. *PLoS Biol.* **12**, e1001805.

6. Gordon DM. 2021 Measuring collective behavior: an ecological approach. *Theory Biosci.* **140**, 353–360.

7. King AJ, Fehlmann G, Biro D, Ward AJ, Fürtbauer I. 2018 Re-wilding Collective Behaviour: An Ecological Perspective. *Trends Ecol. Evol.* **33**, 347–357.

8. Sheppard LW, Mechtley B, Walter JA, Reuman DC. 2020 Self-organizing cicada choruses respond to the local sound and light environment. *Ecol. Evol.* **10**, 4471–4482.

9. Ouellette NT, Gordon DM. 2021 Goals and Limitations of Modeling Collective Behavior in Biological Systems. *Frontiers in Physics* **9**. (doi:10.3389/fphy.2021.687823)

10. Dibnah AJ, Herbert-Read JE, Boogert NJ, McIvor GE, Jolles JW, Thornton A. 2022 Vocally mediated consensus decisions govern mass departures from jackdaw roosts. *Curr. Biol.* **32**, R455–R456.

11. Garnier S, Gautrais J, Theraulaz G. 2007 The biological principles of swarm intelligence. *Swarm Intelligence* **1**, 3–31.

12. Acebrón JA, Bonilla LL, Pérez Vicente CJ, Ritort F, Spigler R. 2005 The Kuramoto model: A simple paradigm for synchronization phenomena. *Reviews of Modern Physics*. **77**, 137–185. (doi:10.1103/revmodphys.77.137)

13. Araujo SBL, Rorato AC, Perez DM, Pie MR. 2013 A spatially explicit model of synchronization in fiddler crab waving displays. *PLoS One* **8**, e57362.

14. Rathore A, Isvaran K, Guttal V. 2023 Lekking as collective behaviour. *Philos. Trans. R. Soc. Lond. B Biol. Sci.* **378**, 20220066.

15. Buck J, Buck E. 1978 Toward a Functional Interpretation of Synchronous Flashing by Fireflies. *Am. Nat.* **112**, 471–492.

16. Legett HD, Page RA, Bernal XE. 2019 Synchronized mating signals in a communication network: the challenge of avoiding predators while attracting mates. *Proc. Biol. Sci.* **286**, 20191067.

17. Greenfield MD, Aihara I, Amichay G, Anichini M, Nityananda V. 2021 Rhythm interaction in animal groups: selective attention in communication networks. *Philos. Trans. R. Soc. Lond. B Biol.*

Sci. **376**, 20200338.

18. Greenfield MD. 2005 Displays in Arthropods and Anurans. *Adv. Stud. Behav.* **35**, 1.

19. Greenfield MD, Tourtellot MK, Snedden WA. 1997 Precedence effects and the evolution of chorusing. *Proceedings of the Royal Society of London. Series B: Biological Sciences* **264**, 1355–1361.

20. McLellan CF, Montgomery SH. 2023 Towards an integrative approach to understanding collective behaviour in caterpillars. *Philos. Trans. R. Soc. Lond. B Biol. Sci.* **378**, 20220072.

21. Ramaswamy K, Cocroft RB. 2009 Collective signals in treehopper broods provide predator localization cues to the defending mother. *Anim. Behav.* **78**, 697–704.

22. Hartbauer M, Siegert ME, Fertschai I, Römer H. 2012 Acoustic signal perception in a noisy habitat: lessons from synchronising insects. *J. Comp. Physiol. A Neuroethol. Sens. Neural Behav. Physiol.* **198**, 397–409.

23. Nityananda V, Balakrishnan R. 2021 Synchrony of complex signals in an acoustically communicating katydid. *J. Exp. Biol.* (doi:10.1242/jeb.241877)

24. Backwell P, Jennions M, Passmore N, Christy J. 1998 Synchronized courtship in fiddler crabs. *Nature* **391**, 31–32.

25. Backwell PRY. 2019 Synchronous waving in fiddler crabs: a review. *Curr. Zool.* **65**, 83–88.

26. Buck J, Buck E. 1976 Synchronous fireflies. *Sci. Am.* **234**, 74–9, 82–5.

27. Sarfati R, Hayes JC, Peleg O. 2021 Self-organization in natural swarms of Photinus carolinus synchronous fireflies. *Sci Adv* **7**. (doi:10.1126/sciadv.abg9259)

28. Buck J. 1988 Synchronous rhythmic flashing of fireflies. II. *Q. Rev. Biol.* **63**, 265–289.

29. Buck J, Buck E. 1968 Mechanism of rhythmic synchronous flashing of fireflies. Fireflies of Southeast Asia may use anticipatory time-measuring in synchronizing their flashing. *Science* **159**, 1319–1327.

30. Morin JG. 1986 Firefleas of the Sea: Luminescent Signaling in Marine Ostracode Crustaceans. *Fla. Entomol.* **69**, 105–121.

31. Ellis EA *et al.* 2022 Sexual signals persist over deep time: ancient co-option of bioluminescence for courtship displays in cypridinid ostracods. *Syst. Biol.* (doi:10.1093/sysbio/syac057)

32. Brock TD. 1970 High Temperature Systems. *Annu. Rev. Ecol. Syst.* **1**, 191–220.

33. Vandekerkhove J, Martens K, Rossetti G, Mesquita-Joanes F, Namiotko T. 2013 Extreme tolerance to environmental stress of sexual and parthenogenetic resting eggs ofEucypris virens(Crustacea, Ostracoda). *Freshw. Biol.* **58**, 237–247.

34. Oakley TH. 2005 Myodocopa (Crustacea: Ostracoda) as models for evolutionary studies of light and vision: multiple origins of bioluminescence and extreme sexual dimorphism. *Hydrobiologia* **538**, 179–192.

35. Cohen AC, Morin JG. 2003 Sexual Morphology, Reproduction and the Evolution of Bioluminescence in Ostracoda. *The Paleontological Society Papers* **9**, 37–70.

36. Morin JG. 2019 Luminaries of the reef: The history of luminescent ostracods and their courtship displays in the Caribbean. *J. Crustacean Biol.* **39**, 227–243.

37. Morin JG, Cohen AC. 2010 It's All About Sex: Bioluminescent Courtship Displays, Morphological Variation and Sexual Selection in Two New Genera of Caribbean Ostracodes. *J. Crustacean Biol.* **30**, 56–67.

38. Rivers TJ, Morin JG. 2008 Complex sexual courtship displays by luminescent male marine ostracods. *J. Exp. Biol.* **211**, 2252–2262.

39. Hensley NM *et al.* 2021 Selection, drift, and constraint in cypridinid luciferases and the diversification of bioluminescent signals in sea fireflies. *Mol. Ecol.* **30**, 1864–1879.

40. Gerrish GA, Morin JG. 2016 Living in sympatry via differentiation in time, space and display characters of courtship behaviors of bioluminescent marine ostracods. *Mar. Biol.* **163**, 190.

41. Rivers TJ, Morin JG. 2013 Female ostracods respond to and intercept artificial conspecific male luminescent courtship displays. *Behav. Ecol.* **24**, 877–887.

42. Torres E, Morin JG. 2007 Vargula Annecohenae, a New Species of Bioluminescent Ostracode (Myodocopida: Cypridinidae) from Belize. *J. Crustacean Biol.*

43. Cohen AC, Morin JG. 2010 Two New Bioluminescent Ostracode Genera, Enewton And Photeros (Myodocopida: Cypridinidae), with Three New Species from Jamaica. *J. Crustacean Biol.* **30**, 1–55.

44. Rivers TJ, Morin JG. 2009/9 Plasticity of male mating behaviour in a marine bioluminescent ostracod in both time and space. *Anim. Behav.* **78**, 723–734.

45. Gerrish GA, Morin JG, Rivers TJ, Patrawala Z. 2009 Darkness as an ecological resource: the role of light in partitioning the nocturnal niche. *Oecologia* **160**, 525–536.

46. Torres E, Cohen AC. 2005 Vargula morini, a new species of bioluminescent ostracode (Myodocopida: Cypridinidae) from Belize and an associated copepod (Copepoda: Siphonostomatoida: Nicothoidae). *J. Crustacean Biol.* **25**, 11–24.

47. Sarfati R, Gaudette L, Cicero JM, Peleg O. 2022 Statistical analysis reveals the onset of synchrony in sparse swarms of Photinus knulli fireflies. *J. R. Soc. Interface* **19**, 20220007.

48. Huvard AL. 1993 Analysis of visual pigment absorbance and luminescence emission spectra in marine ostracodes (Crustacea: Ostracoda). *Comp. Biochem. Physiol. A Physiol.* **104**, 333–338.

49. Raible F, Takekata H, Tessmar-Raible K. 2017 An Overview of Monthly Rhythms and Clocks. *Front. Neurol.* **8**, 189.

50. Morin JG. 1983 Coastal Bioluminescence: Patterns and Functions. *Bull. Mar. Sci.* **33**, 787–817.

51. Kahn AT, Holman L, Backwell PRY. 2014 Female preferences for timing in a fiddler crab with synchronous courtship waving displays. *Anim. Behav.* **98**, 35–39.

52. Nguyen DMT, Iuzzolino ML, Mankel A, Bozek K, Stephens GJ, Peleg O. 2021 Flow-mediated

olfactory communication in honeybee swarms. *Proc. Natl. Acad. Sci. U. S. A.* **118**. (doi:10.1073/pnas.2011916118)

53. Greenfield MD, Roizen I. 1993 Katydid synchronous chorusing is an evolutionarily stable outcome of female choice. *Nature* **364**, 618–620.

54. Poel W, Daniels BC, Sosna MMG, Twomey CR, Leblanc SP, Couzin ID, Romanczuk P. 2022 Subcritical escape waves in schooling fish. *Sci Adv* **8**, eabm6385.

55. Moiseff A, Copeland J. 2010 Firefly synchrony: a behavioral strategy to minimize visual clutter. *Science* **329**, 181.

56. Moen RA, Pastor J, Cohen Y. 1999 Antler growth and extinction of Irish elk. *Evol. Ecol. Res.* **1**, 235–249.

57. Greenfield MD, Honing H, Kotz SA, Ravignani A. 2021 Synchrony and rhythm interaction: from the brain to behavioural ecology. *Philos. Trans. R. Soc. Lond. B Biol. Sci.* **376**, 20200324.

58. Doyle JC, Csete M. 2011 Architecture, constraints, and behavior. *Proc. Natl. Acad. Sci. U. S. A.* **108 Suppl 3**, 15624–15630.

59. Papadopoulou M, Fürtbauer I, O'Bryan LR, Garnier S, Georgopoulou DG, Bracken AM, Christensen C, King AJ. 2023 Dynamics of collective motion across time and species. *Philos. Trans. R. Soc. Lond. B Biol. Sci.* **378**, 20220068.

60. Cohen AC, Morin JG. 1986 *Three new luminescent ostracodes of the genus Vargula (Myodocopida, Cypridinidae) from the San Blas region of Panama*. Natural History Museum of Los Angeles County.

61. Bittman EL. 2021 Entrainment Is NOT Synchronization: An Important Distinction and Its Implications. *J. Biol. Rhythms* **36**, 196–199.

62. Carlson AD, Copeland J. 1985 Flash Communication in Fireflies. *Q. Rev. Biol.* **60**, 415–436.

63. Cohen AC, Oakley TH. 2017 Collecting and processing marine ostracods. *J. Crustacean Biol.* **37**, 347–352.

64. Hensley Nicholai M., Ellis Emily A., Gerrish Gretchen A., Torres Elizabeth, Frawley John P., Oakley Todd H., Rivers Trevor J. 2019 Phenotypic evolution shaped by current enzyme function in the bioluminescent courtship signals of sea fireflies. *Proceedings of the Royal Society B: Biological Sciences* **286**, 20182621.

65. Escobar-Camacho D, Pierotti MER, Ferenc V, Sharpe DMT, Ramos E, Martins C, Carleton KL. 2019 Variable vision in variable environments: the visual system of an invasive cichlid (Cichla monoculus) in Lake Gatun, Panama. *J. Exp. Biol.* **222**. (doi:10.1242/jeb.188300)

66. Brown D, Cox AJ. 2009 Innovative Uses of Video Analysis. *Phys. Teach.* **47**, 145–150.

67. Wilke CO. 2019 *Fundamentals of Data Visualization: A Primer on Making Informative and Compelling Figures*. 'O'Reilly Media, Inc.'

68. Okabe M, Ito K. In press. Color universal design (cud)-how to make figures and presentations that are friendly to colorblind people. *Retrieved April*

69. Anderson MJ, Robinson J. 2001 Permutation tests for linear models. *Aust. N. Z. J. Stat.* **43**, 75–88.

70. Wickham H, Wickham MH. In press. Package tidyverse. *the 'Tidyverse*

71. Wickham H. 2011 Ggplot2. *Wiley Interdiscip. Rev. Comput. Stat.* **3**, 180–185.

72. Wickham H, Bryan J. In press. readxl: Read excel files. *R package version*

73. Neuwirth E, Neuwirth ME. 2014 Package 'RColorBrewer'. *ColorBrewer Palettes*

74. Aphalo PJ. In press. ggpmisc: Miscellaneous Extensions to 'ggplot2'. *R package version 0.3*

75. Kassambara A. In press. ggpubr:'ggplot2' based publication ready plots (Version 0.1. 7). *desde https://CRAN. R-project. org/package= ggpubr*

76. Wickham H, François R, Henry L, Müller K. In press. dplyr: A grammar of data manipulation. *R package version 0.4*

77. Attali D, Baker C. In press. ggExtra: Add marginal histograms to 'ggplot2', and more 'ggplot2'enhancements. *R package version*

78. Ripley B, Venables B, Bates DM, Hornik K, Gebhardt A, Firth D, Ripley MB. 2013 Package 'mass'. *Cran r* **538**, 113–120.

79. Kremer LPM. 2019 ggpointdensity: A cross between a 2D density plot and a scatter plot.

80. Wickham H, Wickham MH. 2017 Package 'tidyr'. *Easily Tidy Data with'spread'and'gather ()'Functions*

81. Pedersen TL. 2019 Package 'patchwork'. *R package http://CRAN. R-project. org/package= patchwork. Cran*

82. Urbanek S. In press. png: Read and write PNG images. *R package version 0.1-7*

83. Baddeley A, Turner R. 2005 spatstat: An R Package for Analyzing Spatial Point Patterns. *J. Stat. Softw.* **12**, 1–42.

84. Robinson D. 2014 broom: An R Package for Converting Statistical Analysis Objects Into Tidy Data Frames. *arXiv [stat.CO]*.

85. Wickham H. 2010 Stringr: Modern, consistent string processing. *R J.* **2**, 38.

86. Xu S, Chen M, Feng T, Zhan L, Zhou L, Yu G. 2021 Use ggbreak to Effectively Utilize Plotting Space to Deal With Large Datasets and Outliers. *Front. Genet.* **12**, 774846.

87. Lüdecke D, Ben-Shachar M, Patil I, Waggoner P, Makowski D. 2021 Performance: An R package for assessment, comparison and testing of statistical models. *J. Open Source Softw.* **6**, 3139.

88. Lüdecke D. In press. sjPlot: Data visualization for statistics in social science. *R package version*

89. Long JA. In press. jtools: Analysis and presentation of social scientific data. *R package version*

90. Lenth R, Singmann H, Love J, Buerkner P, Herve M. 2019 Package 'emmeans'.

91. Hothorn T, Bretz F, Hothorn MT. In press. The multcomp package. *The R Project for Statistical Computing*

92. Graves S, Piepho HP, Selzer L, Dorai-Raj S. In press. multcompView: Visualizations of Paired Comparisons. R package version 0.1-7. *R Found. Stat. Comput., Vienna, Austria*

93. Wickham H, Wickham MH, RColorBrewer I. 2016 Package 'scales'. *R package version* **1**.

94. Schloerke B, Crowley J, Cook D, Briatte F, Marbach M. In press. GGally: extension to 'ggplot2'. R package version 1.4. 0. *R Foundation for Statistical*

95. Rivers TJ, Morin JG. 2012 The relative cost of using luminescence for sex and defense: light budgets in cypridinid ostracods. *J. Exp. Biol.* **215**, 2860–2868.

96. Cohen AC, Morin JG. 1993 The cypridinid copulatory limb and a new genus Kornickeria (Ostracoda: Myodocopida) with four new species of bioluminescent ostracods from the Caribbean. *Zool. J. Linn. Soc.* **108**, 23–84.

97. Electronic supplementary information for Hensley et al. 2023. Collective synchrony of mating signals modulated by ecological cues and social signals in bioluminescent sea fireflies. https://github.com/NikoHensley/ESM_egd_collective_behavior